Resonant vibrational excitation of H₂ by electron impact: Full-range differential cross sections

G. B. Poparić[*] and D. S. Belić

University of Belgrade, Faculty of Physics, Studentski trg 12-16, P.O. Box 368, 11000 Belgrade, Serbia

M. M. Ristić

University of Belgrade, Faculty of Physical Chemistry, Studentski trg 12-16, P.O. Box 137, 11000 Belgrade, Serbia
(Received 19 April 2010; published 22 July 2010)

Electron-impact vibrational excitation of the hydrogen molecule has been revisited in the energy region from 1 to 5 eV. A crossed-beam double trochoidal electron spectrometer is used. Forward and backward scattered electrons from the $v = 0 \rightarrow 1$ excitation channel are separated by electron-beam modulation and time-of-flight detection technique. Present results are normalized and absolute values of differential cross sections at critical border angles of 0° and 180° are determined. In this way the differential cross-section measurements are completed in the full angular range from 0° to 180°.

PACS number(s): 34.80.Gs

I. INTRODUCTION

Molecular hydrogen, as the most fundamental of all electron-molecule scattering systems, has been the subject of numerous experimental and theoretical studies. They have been summarized in review articles by Schulz in 1973 [1], Trajmar *et al.* in 1983 [2], and more recently by Brunger and Buckman in 2002 [3]. The first observation of a large vibrational-excitation cross section in H₂ was due to Ramien in 1931 [4] at 3.5 and 7 eV, and this was confirmed by Engelhardt and Phelps [5] and Schulz [6]. The angular-distribution measurements of Ehrhardt *et al.* [7], performed in the range from 10° to 120° on electrons having excited the $v = 1$ vibrational state of H₂, show a p-wave character (minimum at 90°) and thus confirm the $^2\Sigma_u^+$ designation for this shape resonance.

Linder and Schmidt [8] and Wong and Schulz [9] have applied beam experiment with a sufficient energy resolution to resolve rotational structure associated with vibrational excitation. Differential cross sections (DCSs) for individual vibrational-rotational excitations were measured in the range from 20° to 120°. The results were extrapolated into full angular range and integral cross sections (ICS) are determined.

Crompton *et al.* [10] and England *et al.* [11] obtained $v = 0 \rightarrow 1$ integral vibrational-excitation cross sections from swarm experiments. A significant disagreement between the beam results [7] and the swarm data [10,11] is found, in particular, in the near-threshold energy region. This discrepancy has been the subject of further experimental and theoretical effort for many years.

Morrison *et al.* [12] carried out a number of vibrational close-coupling calculations on electron-hydrogen scattering and their results for the integral $v = 0 \rightarrow 1$ cross section largely agreed with the crossed-beam experiments. A similar situation is apparent from the complex Kohn calculations of Rescigno *et al.* [13].

Nishimura *et al.* [14] also measured differential cross sections in the range from 20° to 120° and derived integral cross sections for the $v = 0 \rightarrow 1$ excitation at energies

above 2.5 eV, which were in reasonably good agreement with the previous results [7,8]. Allan [15] measured the energy dependence of the forward plus backward differential vibrational-excitation ($v = 0 \rightarrow 1 - 6$) cross sections using a trochoidal spectrometer. Although it is not clear that the comparison is fully appropriate, he found that the energy dependence of the cross sections for the first three vibrational levels were in good agreement with those of Ehrhardt *et al.* [7].

A series of absolute elastic and vibrational-excitation cross-section measurements and scattering calculations were performed by Buckman *et al.* [16] and Brunger *et al.* [17]. These experiments, which involved measurements of the ratios of vibrational excitation to elastic scattering, were placed on an absolute scale by the use of the relative flow technique and a careful characterization of the transmission for elastic and inelastic electrons. Absolute differential cross sections are determined for energies from 1 to 5 eV and in the angular range from 5° to 130°. These measurements are with a lower uncertainty, so far, and are in qualitatively good agreement with the vibrational close-coupling calculations with a separable representation of exchange [17].

More recently, a new generation of swarm experiments has been implemented by Schmidt *et al.* [18] to measure transport parameters (drift velocity and diffusion coefficients) in both pure electric and crossed electric and magnetic fields. The vibrational-excitation cross sections derived from these measurements are higher than the previous swarm results above 0.6 eV, narrowing the difference between the beam and swarm cross sections.

In the present experiment, electron-impact vibrational excitation of the hydrogen molecule has been investigated with the aim to determine DCSs at border angles of 0° and 180°.

II. EXPERIMENTAL SETUP

Present measurements are performed by using a modified crossed-beam double trochoidal electron spectrometer. The experiment has been described elsewhere [19,20], and only a brief summary will be presented here. The electrons are extracted from a directly heated hairpin tungsten cathode. The monoenergetic electron beam is selected by a trochoidal

---

[*]Goran_Poparic@ff.bg.ac.rs

electron monochromator (TEM) device and collimated into the interaction region. The electron beam is crossed at right angles with the gas beam. After the collision, electrons scattered in a forward (and backward) direction are analyzed by use of a double TEM device [19–22] and detected by a channel electron multiplier.

In the originally designed apparatus, the detected signal consists of the sum of electrons inelastically scattered at 0° and 180°, within the same solid angles, at the given residual energy. The collection of the backward scattered electrons, which are reflected on the potential barrier at the monochromator exit, is found to be very efficient (100%). This is due to the presence of a longitudinal magnetic field, needed for the TEM operation, and has been demonstrated by Allan [21], Asmis and Allan [22], and Poparic *et al.* [23].

Electrons scattered at 0° travel straight to the analyzer system and to the detector. On the other side, inelastic electrons scattered at 180° move backward along the incident electron-beam trajectory, are reflected at the potential barrier on the electrode in front of the collision chamber, reach again the collision region, and from there follow the same path as the forward scattered electrons. Thus, they travel a longer distance and need a longer time to reach the detector. This fact is used to separate these two groups of electrons by recording their time-of-flight spectra.

For this kind of measurement, the incident electron beam needs to be pulsed in an appropriate way [21–23]. In the present experiment, electron-beam chopping is enabled by a 1.18-MHz square-shaped asymmetric pulse generator. Square pulses of 50 ns, 2-V high, are separated by 800 ns. This signal is superimposed on one of the monochromator electrodes. The potential of this electrode keeps the electron beam on during 50 ns of the pulse time and off for the rest of the time.

Since the collision can occur only during the pulse on time, the rising time of the pulses can be used as a trigger of the time-to-amplitude converter (TAC). In fact, this signal is used as a stop trigger of the TAC. For the start of the TAC, the signal from the channeltron is used. Therefore, each recorded event represents the time difference between electron detection and the next pulse coming from the generator. This inverted configuration has no influence on the results, but increases the detection efficiency of the experiment.

This procedure has been successfully applied to separate forward and backward scattered electrons from the $E^3\Sigma_g^+$ state excitation of the N$_2$ molecule [20]. Measurements were performed near threshold, with very low residual electron energy of 67 meV only. In the case of slow electrons, the time difference between detection of forward and backward electrons is sufficient to separate these two groups. For faster, more energetic electrons, however, backward scattered electrons reflect quickly and follow very closely forward scattered ones and the two contributions overlap in time. Therefore, electrons scattered backward with higher energy need to be decelerated and to travel some distance with low velocity, before they get back to the collision region. In that way, the time difference of their arrival to the detector can be increased. For this purpose a decelerator device has been introduced in front of the collision region. It consists of two parallel plates, 20-mm long. They are kept at low negative potential below the interaction region so that backward scattered electrons

travel with low velocity back and forth over this distance and spend some 80–100 ns in this device, before entering again the collision region from the opposite direction. The operation of the decelerator device has been successfully tested and applied in our experiment on the CO molecule [23].

The signal from the channeltron is processed by a fast charge amplifier, voltage amplifier, and high-voltage filter. Obtained pulses are used for the start signal of the TAC. The signal from the TAC is loaded to a pulse-height analyzer (PHA) and multichannel analyzer (MCA). Obtained time-of-flight spectra are analyzed by an online computer.

In order to check detection efficiency and focusing properties of our experimental setup, measurements are first performed on the $^2\Pi_g$ resonance in the N$_2$ molecule. The angular distribution of the scattered electrons, according to its symmetry, is given by a simple $d\pi$ wave. Thus, it is symmetric relative to 90°, dominated by forward and backward peaks, with a local maximum at 90° [3]. In our measurements, the ratio of forward-to-backward signal is found to be (1.00 ± 0.05). A similar experiment also has been performed for electrons scattered by the $^2\Pi$ resonance in CO. The ratio of forward-to-backward signal is confirmed to be (1.00 ± 0.05), the same as in our previous measurements [23].

III. RESULTS AND DISCUSSION

Measurements are performed for the $v = 0 \rightarrow 1$ vibrational level excitation for incident electron energies (E_e) of 1.0, 1.5, 2.5, and 5.0 eV, respectively. Typical time-of-flight spectrum is illustrated in Fig. 1 for incident electron energy of 2.5 eV. As can be seen from the figure, the spectrum consists of two distinct peaks on the timescale. The first, narrower one, at 440 ns, belongs to the electrons scattered at 0°, directly to the analyzer and detector. The second, broader peak, around 580 ns, corresponds to electrons scattered at 180°, which are decelerated, reflected by the monochromator potential barrier, and detected somewhat delayed in time. The two peaks are separated for more than 100 ns. The ratio of differential cross sections at 0° and at 180° is proportional to the ratios of the
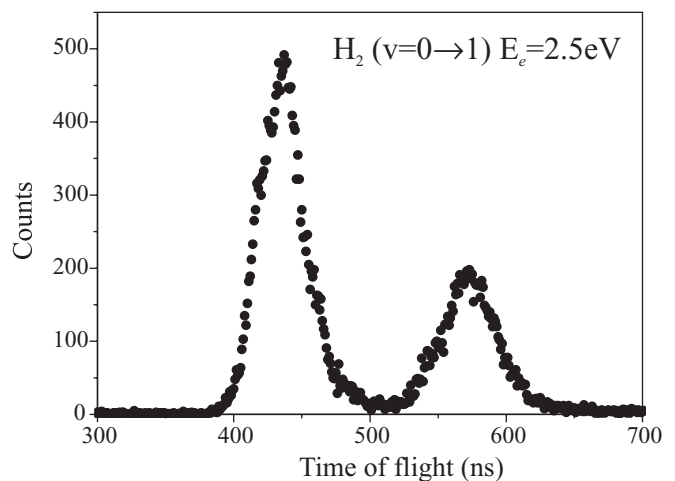

FIG. 1. Time-of-flight spectrum of electrons scattered at 0° and 180° from the $v = 1$ level excitation in H$_2$, at incident energy of 2.5 eV.

TABLE I. DCS and ICS for the $v = 0 \rightarrow 1$ vibrational excitation of H_2 by electron impact.

E_e (eV)	DCS ratio $0°/180°$	DCS $(10^{-18} cm^2 sr^{-1})$		ICS $(10^{-18} cm^2)$
		$0°$	$180°$	
1.0	1.54	1.59	1.03	7.8
1.5	1.97	4.97	2.52	26.7
2.5	2.01	9.14	4.55	39.5
5.0	1.33	8.02	6.03	32.7

areas under these two peaks. In this specific case, forward-to-backward ratio is found to be equal to (2.01 ± 0.10).

Present results for the ratio of forward-to-backward scattered electrons, for vibrational excitation of the $v = 0 \rightarrow 1$ level excitation of H_2, are presented in Table I. They are found to be 1.54, 1.97, 2.01, and 1.33, for electron energies of 1.0, 1.5, 2.5, and 5.0 eV, respectively. The estimated statistical error bar is found to be of the order of $\pm 5\%$.

Present results are placed on an absolute scale of the differential cross section by performing normalization to the most recent and more complete DCS values reported by Brunger *et al.* [17], which cover the range from $5°$ to $130°$. First, extrapolation of Brunger's DCS to $0°$ is performed by the Legendre polynomials. In this way the initial value of DCS at $0°$ is obtained. For some cases, extrapolation is considered in the angular interval of $5°$ only, and for others in $20°$. Secondly, by using present forward-to-backward DCS ratio, the DCS value at $180°$ is determined, for each of the considered electron energies. By using fourth-order Legendre polynomials, successive interpolation procedure is applied to the complete set of data, which consists of the present data at $0°$ and $180°$ and of the results of Brunger *et al.* [17]; in that way the overall angular distribution is determined. The DCS values, obtained for $0°$ and $180°$, are presented in Table I, and are also shown in Figs. 2–5 for electron energies of 1.0, 1.5, 2.5, and 5.0 eV, respectively. The last fit of the data is also shown in the figures.
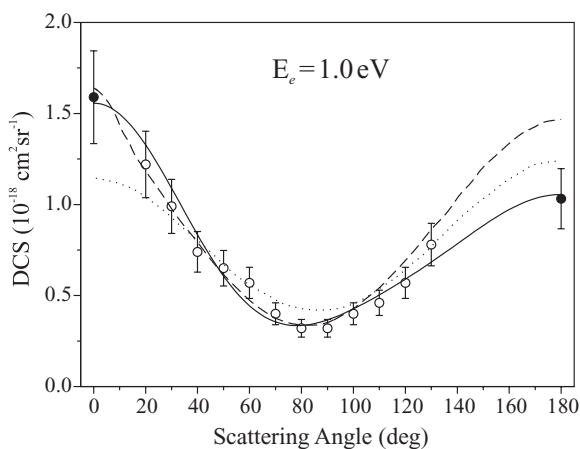

FIG. 3. DCS for $v = 0 \rightarrow 1$ of H_2 at 1.5 eV. Present results (solid circles); Brunger *et al.* [17] (open circles); Linder and Schmidt [8] (solid triangles); Morrison *et al.* [12] (dashed); Legendre polynomial fit (solid line).

FIG. 4. DCS for $v = 0 \rightarrow 1$ of H_2 at 2.5 eV. Present results (solid circles); Brunger *et al.* [17] (open circles); Linder and Schmidt [8] (solid triangles); Nishimura *et al.* [14] (open triangles); Morrison *et al.* [12] (dashed); Rescigno *et al.* [13] (dotted); Legendre polynomial fit (solid line).

FIG. 2. DCS for $v = 0 \rightarrow 1$ of H_2 at 1.0 eV. Present results (solid circles); Brunger *et al.* [17] (open circles); Morrison *et al.* [12] (dashed); Rescigno *et al.* [13] (dotted); Legendre polynomial fit (solid line).
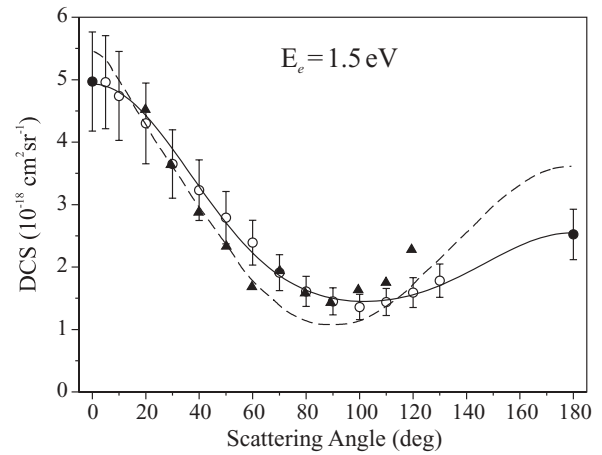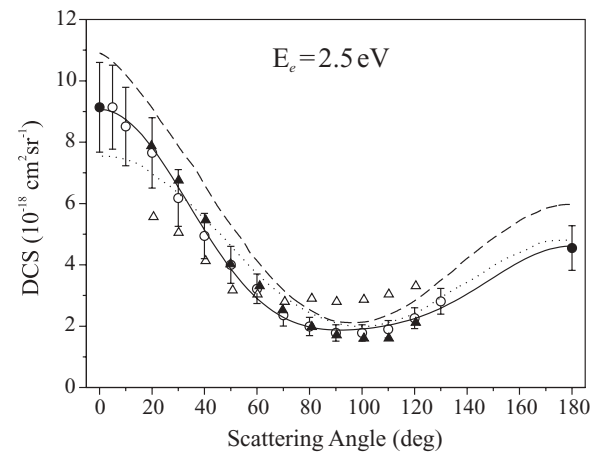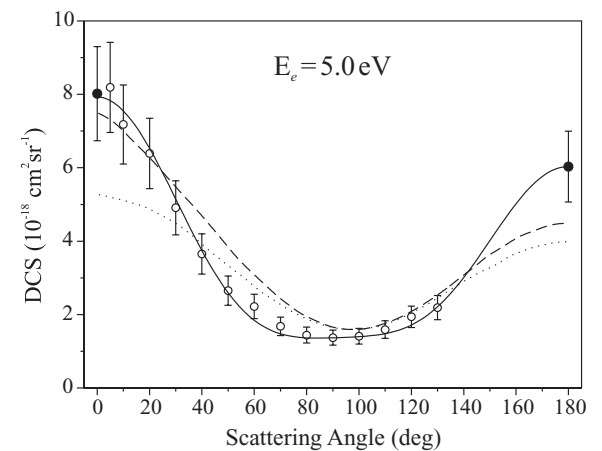

FIG. 5. DCS for $v = 0 \rightarrow 1$ of H_2 at 5.0 eV. Present results (solid circles); Brunger *et al.* [17] (open circles); Morrison *et al.* [12] (dashed); Rescigno *et al.* [13] (dotted); Legendre polynomial fit (solid line).

Estimated errors associated with the present DCS values include error bars of our signal separation procedure (5%), error bars of the data used for normalization (15%) [17], and error from the extrapolation procedure (which is found to be 6% for $E_e = 1.0$ eV and 2% in all other cases, at 90% confidence level). The total uncertainties are found to be 17% in the case of $E_e = 1.0$ eV and 16% in all other cases.

The results of the last fit of the data, presented by the solid lines in Figs. 2–5, are then used as the scattered electrons' angular distribution in order to determine the integral cross sections for the corresponding electron energies. These ICS values are also presented in Table I. Error bars for ICS values are calculated by integrating 90% confidence bands of the polynomial fit. They are found to be 27% for $E_e = 1.0$ eV, and 20% for all other cases.

Present results are compared with other experimental and theoretical results. They are in a fairly good agreement up to the shape of the distribution with most of them, with the minimum around 90° and asymmetric peaks at 0° and 180°, the last being noticeably lower. Present results fit well as a complementary to all experimental data of Brunger *et al.* [17]. For 1.0 eV (Fig. 2), the calculations of Morrison *et al.* [12] are in excellent agreement with the present data at 0° and overestimate them for more than 40% at 180°. The theory of Rescigno *et al.* [13] underestimates our data at low angle and overestimates them at 180° for some 20%, both being nearly symmetric relative to 90°. For 1.5 eV, present data agree well with the measurements of Brunger *et al.* [17] and Linder and Schmidt [8], but again are overestimated by Morrison *et al.* [12] for more than 40% at 180°. A similar situation is seen also for 2.5 and 5.0 eV, except that for 5.0 eV both theoretical predictions of Morrison *et al.* [12] and Rescigno *et al.* [13] underestimate the present result at 180° for 20% and 25%, respectively.

Present ICS values are compared in Fig. 6 with the previous experimental and theoretical results. This comparison is presented both for the crossed-beam experiments and the swarm results. The experimental results in Figs. 2–5. of Brunger *et al.* [17], Linder and Schmidt [8], Nishimura *et al.* [14], Ehrhardt *et al.* [7], England *et al.* [11] and Schmidt *et al.* [18] are included, as well as the predictions of Morrison *et al.* [12] and Rescigno *et al.* [13]. The agreement among different sets of data is satisfactory and within the estimated error bars.
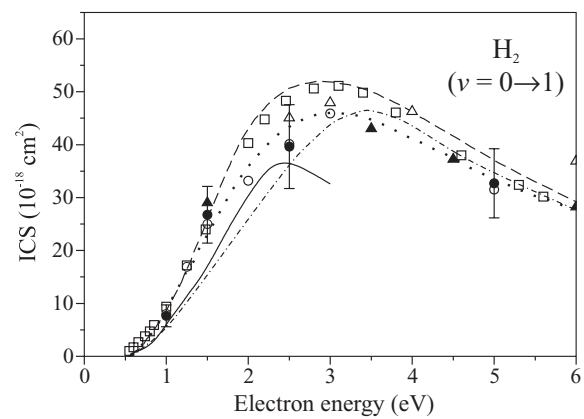

FIG. 6. ICS for $v = 0 \rightarrow 1$ of H_2. Present results (solid circles); Brunger *et al.* [17] (open circles); Linder and Schmidt [8] (solid triangles); Nishimura *et al.* [14] (open triangles); Ehrhardt *et al.* [7] (open squares); Morrison *et al.* [12] (dashed); Rescigno *et al.* [13] (dotted); England *et al.* [11] (dash-dotted); Schmidt *et al.* [18] (solid line).

IV. CONCLUSIONS

Present results have fulfilled a long-standing lack of experimental DCS data and the angular distribution of electrons from vibrational excitation of H_2 at border angles of 0° and 180°. They might be a test for further theoretical development in this field. Existing close-coupling theory with a separable treatment of exchange [12] and complex Kohn calculations [13] are seen to reproduce correctly the overall shape of the vibrational excitation, but still have not predicted well the amplitude for the backward scattered electrons. Furthermore, the possibility of inclusion of the present full-range angular distribution of electrons may initiate more sophisticated Monte Carlo simulations of the hydrogen discharge and gas transport properties, in particular, in the presence of external electric and magnetic fields.

ACKNOWLEDGMENT

[1] G. J. Schulz, Rev. Mod. Phys. **45**, 423 (1973).

[2] S. Trajmar, D. F. Register, and A. Chutjian, Phys. Rep. **97**, 219 (1983).

[3] M. J. Brunger and S. J. Buckman, Phys. Rep. **357**, 215 (2002).

[4] H. Ramien, Z. Phys. **70**, 353 (1931).

[5] A. G. Engelhardt and A. V. Phelps, Phys. Rev. **131**, 2115 (1963).

[6] G. J. Schulz, Phys. Rev. **135**, A988 (1964).

[7] H. L. Ehrhardt, L. Langhans, F. Linder, and H. S. Taylor, Phys. Rev. **173**, 222 (1968).

[8] F. Linder and H. Schmidt, Z. Naturforsch. **26a**, 1603 (1971).

[9] S. F. Wong and G. J. Schulz, Phys. Rev. Lett. **32**, 1089 (1974).

[10] R. W. Crompton, D. K. Gibson, and A. G. Robertson, Phys. Rev. A **2**, 1386 (1970).

[11] J. P. England, M. T. Elford, and R. W. Crompton, Aust. J. Phys. **41**, 573 (1988).

[12] M. A. Morrison, R. W. Crompton, B. C. Saha, and Z. L. Petrović, Aust. J. Phys. **40**, 239 (1987).

[13] T. N. Rescigno, B. K. Elza, and B. H. Lengsfield, J. Phys. B **26**, L567 (1993).

[14] H. Nishimura, A. Danjo, and H. Sugahara, J. Phys. Soc. Jpn. **54**, 1757 (1985).

[15] M. Allan, J. Phys. B: At. Mol. Phys. **18**, L451 (1985).

[16] S. J. Buckman, M. J. Brunger, D. S. Newman, G. Snitchler, S. Alston, D. W. Norcross, M. A. Morrison, B. Saha, G. Danby, and W. Trail, Phys. Rev. Lett. **65**, 3253 (1990).

[17] M. J. Brunger, S. J. Buckman, D. S. Newman, and D. T. Alle, J. Phys. B **24**, 1435 (1991).

[18] B. Schmidt, K. Berkhan, B. Gatz, and M. Moller, Phys. Scr. **53**, 30 (1994).

[19] M. Vićić, G. Poparić, and D. S. Belić, Rev. Sci. Instrum. **69**, 1996 (1998).

[20] G. B. Poparić, M. D. Vićić, and D. S. Belić, Phys. Rev. A **66**, 022711 (2002).

[21] M. Allan, J. Electron Spectrosc. Relat. Phenom. **48**, 219 (1989).

[22] K. R. Asmis and M. Allan, J. Phys. B **30**, 1961 (1997).

[23] G. B. Poparić, S. M. D. Galijaš, and D. S. Belić, Phys. Rev. A **70**, 024701 (2004).